

The q -dependent detrended cross-correlation analysis of stock market

Longfeng Zhao^{a,b,*}, Wei Li^{a,**}, Andrea Fenu^{b,f}, Boris Podobnik^{b,c,d,e}, Yougui Wang^{b,g}, H. Eugene Stanley^b

^aComplexity Science Center & Institute of Particle Physics, Hua-Zhong (Central China) Normal University, Wuhan 430079, China

^bCenter for Polymer Studies and Department of Physics, Boston University, Boston, Massachusetts 02215, USA

^cFaculty of Civil Engineering, University of Rijeka, Rijeka, HR 51000, Croatia

^dZagreb School of Economics and Management, Zagreb, HR 10000, Croatia

^eLuxembourg School of Business, Grand-Duchy of Luxembourg, Luxembourg

^fDepartment of economics and management, University of Cagliari

^gSchool of Systems Science, Beijing Normal University, Beijing 100875, PR China

Abstract

The properties of q -dependent cross-correlation matrices of stock market have been analyzed by using the random matrix theory and complex network. The correlation structures of the fluctuations at different magnitudes have unique properties. The cross-correlations among small fluctuations are much stronger than those among large fluctuations. The large and small fluctuations are dominated by different groups of stocks. We use complex network representation to study these q -dependent matrices and discover some new identities. By utilizing those q -dependent correlation-based networks, we are able to construct some portfolio by those most independent stocks which consistently perform the best. The optimal multifractal order for portfolio optimization is approximately $q = 2$. These results have deepened our understanding about the collective behaviors of the complex financial system.

Keywords: q -dependent detrended cross-correlation, stock market, random matrix theory, correlation-based network, portfolio optimization

1. Introduction

Analysis of cross-correlations between different financial assets has become extremely attractive [1, 2] since the researchers started to report the violation of Efficient Market Hypothesis (EMH). At the very beginning, the cross-correlation analyses have relied on such linear tools as the Pearson correlation, which requires stationary in the data, but real-world financial data sets are rarely stationary. To take into account the non-linearity and non-stationarity in real-world data, new methods based on detrendization have been proposed, among which the most popular has been the detrended fluctuation analysis (DFA)[3]. Motivated by the DFA that is applied for a single time series, its generalization named detrended cross-correlation fluctuation analysis (DCCA) has been proposed to quantify the long-range cross-correlations between a pair of non-stationary signals [4]. DFA and DCCA are subsequently extended by their multifractal versions: MF DFA and MF DCCA, respectively[5–7]. DFA, DCCA and their multifractal counterparts have been applied cross a broad range of systems including biological, financial to physical systems[8–10]. Recently an analog to the Pearson coefficient, the detrended cross-correlation coefficient $\rho(s)$ was introduced in Ref[11]. This coefficient applied to non-stationary signals quantifies the significance level of correlations among fluctuations of detrended non-stationary signals at a given detrending scale s [12]. More recently the DCCA coefficient $\rho(s)$ has been widely used to study the non-linear cross-correlation among financial time series[8, 13–16]. Despite the success of the $\rho(s)$ coefficient, it has some limitations when cross-correlations are quantified among the fluctuations at different magnitude. A more recent extension of the $\rho(s)$, the q -dependent detrended cross-correlation coefficient $\rho(q, s)$, $q \in R$,

*Corresponding author

**Corresponding author

Email addresses: zlfccnu@mails.ccnu.edu.cn (Longfeng Zhao), zlfccnu@bu.edu (Longfeng Zhao), liw@mail.ccnu.edu.cn (Wei Li)

is based on the q -dependent fluctuation functions F_q from MF DFA and MF DCCA[5, 7, 17]. Kwapien et al. recently indicated that this method could be applied to the analysis of empirical data from such natural complex systems as physical, biological, social and financial systems. Our focus here is on financial market.

Here we apply the q -dependent cross-correlation coefficient to quantify the cross-correlation among the return time series of 401 constituent stocks of the S&P 500 index. For those return time series, we generate the q -dependent cross-correlation matrices $C(q, s)$. We calculate the statistical properties of the matrices at different multifractal orders and varying time scales. As when analyzing the Pearson cross-correlation matrix, we analyze the eigenvalue and eigenvector dynamics of the matrices and find that the cross-correlations of stock market fluctuations at different magnitudes exhibit a unique structure and dynamics. The large fluctuations are always dominated by a few industry groups, but the small fluctuations exhibit a different behavior. We then represent the cross-correlations matrices as complex networks and use the planar maximally filtered graph (PMFG) method[18] to construct the correlation-based networks and to analyze their basic topological features. The PMFG networks for small fluctuations are more heterogeneous than those obtained for large fluctuations. Using a centrality metric, we classify stocks as central or peripheral according to their centrality ranking. Applying this to portfolio optimization we find that a portfolio of peripheral stocks has a consistently higher return than one of central and randomly selected stocks.

The paper is organized as follows. In Sec. 2 we introduce the methodology used in this paper. In Sec. 3 we present the data and main empirical results. In Sec. 4, an application to portfolio optimization has been given. The last section provides our conclusions.

2. Methodology

2.1. q -dependent cross-correlation analysis

The q -dependent cross-correlation coefficient can be obtained from the following procedure:

(i) We consider a pair of time series x_i and y_i , $i = 1 \dots l$. We integrated these time series and obtain two new time series

$$\chi^x(k) = \sum_{i=1}^k x_i - \langle x \rangle, k = 1 \dots l, \quad (1)$$

$$\chi^y(k) = \sum_{i=1}^k y_i - \langle y \rangle, k = 1 \dots l. \quad (2)$$

(ii) We divide $\chi^x(k)$ and $\chi^y(k)$ into $2M_s = 2 \times \text{int}(l/s)$ non-overlapping boxes of length s from the beginning and end of two integrated time series. We then calculate the local trends for each segment v ($v = 0, 1, \dots, 2M_s - 1$) by a least-square fit and subtract it from $\chi^x(k)$ and $\chi^y(k)$ to detrend the integrated series. We then find the residual signals X, Y equal to the difference between the integrated signals and the m th-order polynomials $P_{s,v}^{(m)}$ fitted to these signals:

$$X_v(s, i) = \sum_{j=1}^i \chi^x(vs + j) - P_{X,s,v}^{(m)}(j), \quad (3)$$

$$Y_v(s, i) = \sum_{j=1}^i \chi^y(vs + j) - P_{Y,s,v}^{(m)}(j). \quad (4)$$

The covariance and variance of X and Y in a box v are defined:

$$f_{XY}^2(s, v) = \frac{1}{s} \sum_{i=1}^s X_v(s, i) Y_v(s, i), \quad (5)$$

$$f_{ZZ}^2(s, v) = \frac{1}{s} \sum_{i=1}^s Z_v^2(s, i), \quad (6)$$

where Z represents either X or Y .

(iii) We then defined the fluctuation functions of order q and scale s

$$F_{XY}^q(s) = \frac{1}{2M_s} \sum_{v=0}^{2M_s-1} \text{sgn}[f_{XY}^2(s, v)] |f_{XY}^2(s, v)|^{q/2}, \quad (7)$$

$$F_{ZZ}^q(s) = \frac{1}{2M_s} \sum_{v=0}^{2M_s-1} [f_{ZZ}^2(s, v)]^{q/2}. \quad (8)$$

The q -dependent cross-correlation coefficient between x_i and y_i is defined:

$$\rho(q, s) = \frac{F_{XY}^q(s)}{\sqrt{F_{XX}^q(s)F_{YY}^q(s)}}, \quad (9)$$

When $q = 2$ we restore the detrended cross-correlation coefficient of $\rho(s)$ [11]. The q -dependent cross-correlation coefficient is bounded in $[-1, 1]$ when $q \geq 0$. The coefficient can have arbitrary value when $q < 0$. Here we focus on the case when $q > 0$. The exponent q acts as a filter. When $q > 2$ the boxes with large fluctuations contribute to $\rho(q, s)$ the most, but when $q < 2$ the boxes with relatively small values dominate the fluctuation function, thus contribute to $\rho(q, s)$ the most.

2.2. Random matrix theory

Having introduced the q -dependent cross-correlation coefficient, we now construct the cross-correlation matrices $C(q, s)$ at different multifractal orders q and detrending scales s . If we assume the correlation matrices are random, the random matrix theory can be employed as a benchmark to quantify to what extent the properties of q -dependent cross-correlation matrices deviate from the prediction of purely random matrix. The random matrix theory has been widely applied to investigate the collective phenomena in financial markets[2, 1, 19–27]. A comprehensive review is provided in Ref. [28].

We consider a random correlation matrix constructed from time series, e.g., a return time series $r_i, i = 1, \dots, L$

$$C = \frac{1}{L} RR^T, \quad (10)$$

where R is an $N \times L$ matrix containing N return time series r_i of length L with zero mean and unit variance, that are mutually uncorrelated. The probability distribution function of eigenvalues of a random matrix can be written analytically in the limit $N, L \rightarrow \infty$ with a fixed $Q = \frac{L}{N} > 1$

$$P(\lambda) = \frac{Q}{2\pi} \frac{\sqrt{(\lambda_+ - \lambda)(\lambda - \lambda_-)}}{\lambda}, \quad (11)$$

where λ_- and λ_+ are the minimum and maximum eigenvalues of $C(q, s)$. λ_- and λ_+ are given by

$$\lambda_{\pm} = 1 + \frac{1}{Q} \pm 2\sqrt{\frac{1}{Q}}. \quad (12)$$

Equation 11 is exact for Gaussian-distributed matrix elements. If the eigenvalue distributions deviate from the prediction of 11, that signals the existence of mutual correlation in the time series.

We decompose the q -dependent cross-correlation matrices with eigenvalues $\lambda_k, k = 1 \dots N$ and eigenvectors $U_k, k = 1 \dots N$ which provide information about the collective behavior of the stock market. Here we use the inverse participate ratio to quantify the reciprocal of the number of eigenvector components that significantly contribute. The inverse participate ratio (IPR) is defined

$$I_k = \sum_{l=1}^N [u_k^l]^4 \quad (13)$$

Here u_k^l is the l th component of the eigenvector U_k corresponding to eigenvalue λ_k . The meaning of I_k can be illustrated by two limiting cases, (i) a vector with identical components $u_k^l = 1/\sqrt{N}$ has $I_k = 1/N$, whereas (ii) a vector with one component $u_k^l = 1$ and the remainder zero has $I_k = 1$. We also define the participate ratio (PR) as $1/I_k$, which approximately equal to the significant contributors for eigenvalue λ_k . In random matrix theory, the expectation of IPR is

$$\langle I_k \rangle = N \int_{-\infty}^{\infty} [u_k^l]^4 \frac{1}{\sqrt{2\pi N}} \exp\left(-\frac{[u_k^l]^2}{2N}\right) du_k^l = \frac{3}{N}. \quad (14)$$

2.3. Planar maximally filtered graph

As suggested in Ref.[17], we use the complex network approach to analyze the q -dependent cross-correlation matrix. We employ the the planar maximally filtered graph (PMFG) method [18] to construct networks based on correlation matrices $C(q, s)$. The algorithm is implemented as follows,

- (i) Sort all of the $\rho_{ij}(q, s)$ in descending order to obtain an ordered list l_{sort} .
- (ii) Add an edge between nodes i and j based on the order in l_{sort} only when the graph remains planar after the edge is added.
- (iii) A graph $G(q, s)$ is formed with $N_e = 3(N - 2)$ edges under the constraint of planarity.

As described in Ref.[18], PMFGs not only keep the hierarchical organization of the minimum spanning tree (MST) but also generate cliques. We calculate the basic topological parameters such as clustering coefficient C , the shortest-path length L and the assortativity A . We also adopt a heterogeneity index γ [29] to measure the heterogeneity of PMFGs which is defined by

$$\gamma = \frac{N - 2 \sum_{ij \in \{e\}} (k_i k_j)^{-1/2}}{N - 2\sqrt{N - 1}}, \quad (15)$$

Here k_i and k_j are the degrees of nodes i and j connected by edge $\{e_{ij}\}$.

3. Data and Results

3.1. Data description

Our data sets include $N = 401$ S&P500 constituent stocks from 4 January 1999 to 31 December 2014 with 4025 trading records for each stock. We use the logarithm return defined as

$$r_i(t) = \ln p_i(t + 1) - \ln p_i(t), \quad (16)$$

where $p_i(t)$ is the daily adjusted closure price of stock i at time t . We then use the previous method to compute the q -dependent cross-correlation coefficients between any pair of return time series $r_i(t)$ and $r_j(t)$ and obtain the $N \times N$ matrix $C(q, s)$. The matrix entries of $C(q, s)$ are the correlation coefficients $\rho_{ij}(q, s)$ between all pairs of stocks. We set $q \in [0.2, 5]$ with $\delta q = 0.2$ and the detrending scale $s \in [30, 1000]$ trading days with $\delta_s = 40$. We also perform the same calculation on the shuffled return time series and the simulated random time series and use them as reference models.

3.2. Cross-correlation matrix analysis

With a series of cross-correlation matrices $C(q, s)$ at different order q and detrending scale s , we analyze the probability distribution of the cross-correlation values, i.e, the upper triangle entries of the correlation matrices.

First we show the plot of matrices for different multifractal order q and detrending scale s in Fig 1, set the diagonal entries to zero for better visualization. The strength of the average correlation will increase slightly as the scale s increases, but will decrease as the multifractal order q increases. We sort the rows and columns of the correlation matrices according to the official sector and subsector partitions of S&P500. Note the distinct sector and subsector structures in the correlation matrices. When $q < 2$ the sector structure is much more pronounced.

Fig2 shows the distribution of the matrices elements $P(\rho)$ for six different values of q and six different values of scale s . We can observe that the distribution of the matrices become increasingly skewed to the left and the

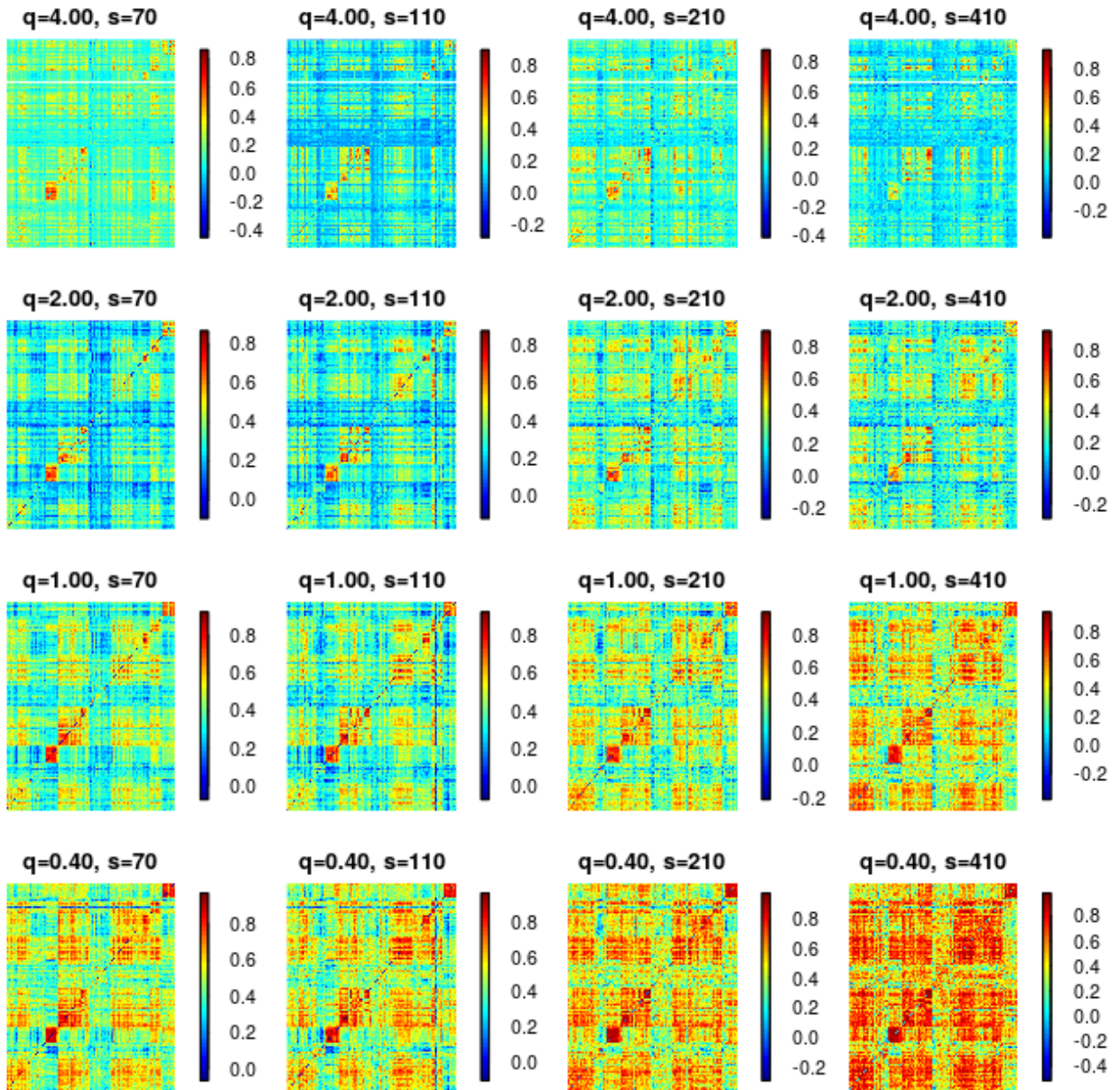


Figure 1: (Color on line) The cross-correlation matrices for different order q and scale s . The diagonal elements have been set to zero.

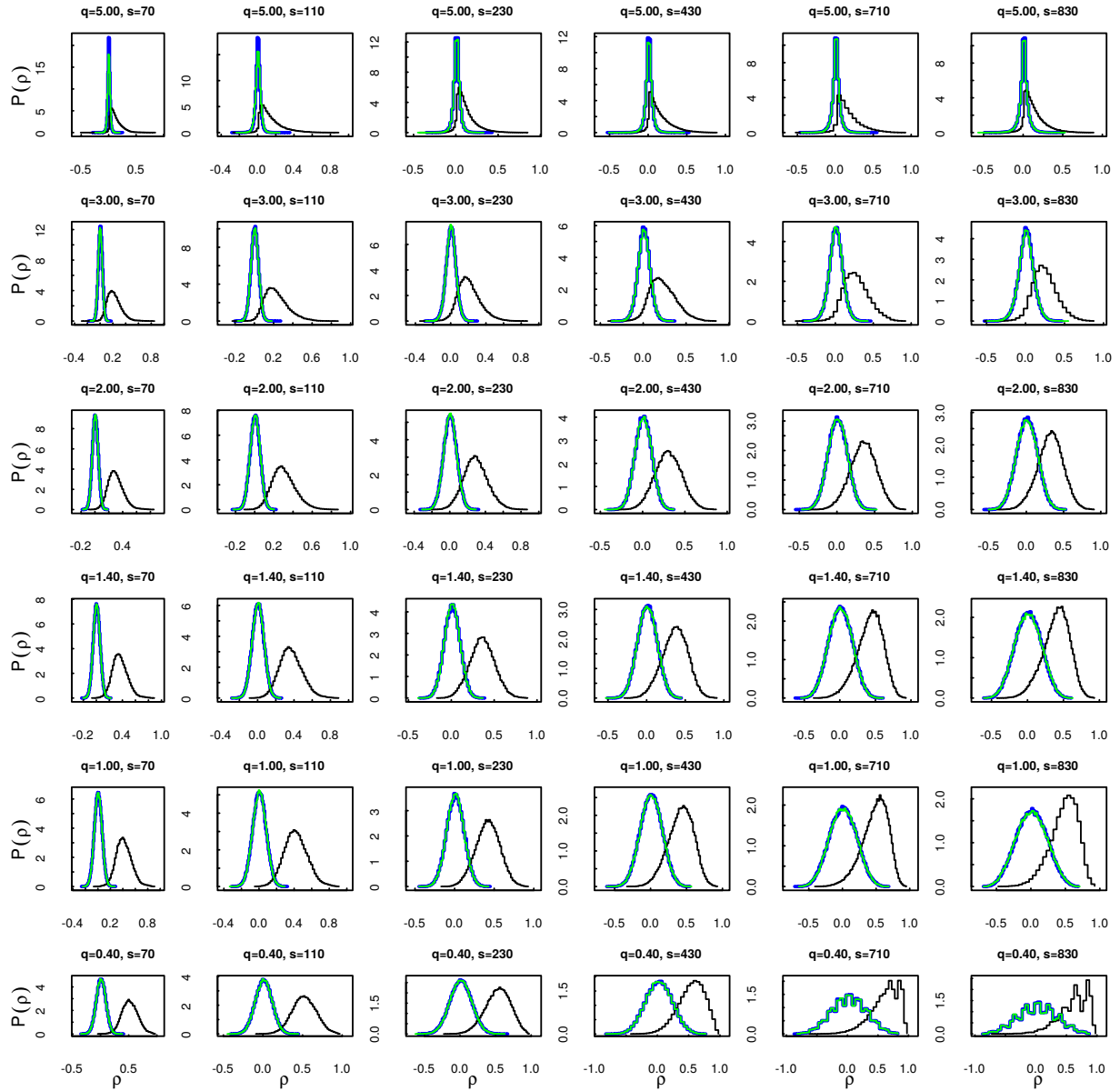


Figure 2: (Color on line) The distribution of the non-diagonal elements of the cross-correlation matrices. The black lines are the distribution of the q -dependent cross-correlation for the return time series. The blue lines and green lines are the same distribution for the shuffled return time series and simulated random time series, respectively.

width of the distribution peaks as the multifractal order q increases. The probability distribution of the q -dependent cross-correlation coefficient for the return time series deviate significantly from the shuffled distribution, and this may provide genuine information about the cross-correlation among different magnitude of fluctuations. The shuffled and simulated distributions are coincide with each other. Thus the different cross-correlation structure is the result of the non-linear correlation among different magnitude of fluctuations. In addition, when $q > 2$ the distribution becomes relatively close to the shuffled case. We calculate the first four order moments of the correlation matrices to illustrate the variation in the cross-correlation distribution.

Fig. 3 shows the first four order moments of the correlation coefficient distribution at different multifractal orders q and detrending scales s . The average cross-correlation decreases as the multifractal order increases, indicating that the cross-correlation between large fluctuations are relatively weak. From the variance, skewness and kurtosis we see an obvious transition in the distribution. The cross-correlation coefficients for large and small multifractal orders q are largely different, which indicate disparate correlation structures among different magnitude of fluctuations.

To analyze the genuine information carried by the q -dependent cross-correlation matrices, we decompose the cross-correlation matrices and sort the eigenvalues $\lambda_k, k = 1 \dots 401$ in ascending order with their corresponding eigenvectors $U_k, k = 1 \dots 401$. Fig 4 and Fig 5 show the distributions of the bulk eigenvalues and deviating eigenvalues, respectively. Fig. 4 only gives eigenvalues smaller than 2. The black and blue lines are the eigenvalue distributions for the original q -dependent cross-correlation matrices and the shuffled scenario. The red lines are the eigenvalue distributions predicted by random matrix theory. We also simulate 401 time series using Gaussian distribution. The green lines are the bulk eigenvalues from the q -dependent cross-correlation matrices calculated using the simulated Gaussian time series. We find that the bulk eigenvalue distribution of the shuffling time series and the simulated time series are approximately the same. This confirms that the deviation of the eigenvalue distribution is the result of non-linear cross-correlation. The lower and upper bounds of the eigenvalues predicted by RMT are $\lambda_- = 0.47$ and $\lambda_+ = 1.73$. The distribution of the bulk eigenvalues for the original q -dependent cross-correlation differ from the random matrix theory prediction. Note that when $q > 2$ the bulk eigenvalue distribution for the original cross-correlation matrices and the shuffled matrices approaches the random matrix prediction. Fig. 5 shows the deviating eigenvalues for the original cross-correlation matrices (black), the shuffled results (blue), and the simulated results (green). The behavior of those deviating eigenvalues differs as the values of q and s differ. Large q values and small s values tend to cause more large deviating eigenvalues. Note that the deviating eigenvalues for large $q = 4$ and small $s = 70$ are especially clear. In contrast, when $q = 0.4$ and $s = 830$ only the largest eigenvalue continues to deviate from the shuffled and simulated eigenvalues. This indicates that the small fluctuations only have a very short characteristic time. The long term average effect of small fluctuations equals the noise level. Generally speaking, large multifractal order q and small detrending scale s makes the sector structures (deviating eigenvalues) and market mode (largest eigenvalue) separated from the noise level.

The first four eigenvalues for different multifractal orders q and detrending scales s is shown in Fig 6. The largest eigenvalues for $q < 2$ are approximately equal to the order of the system size. The behavior of the largest eigenvalues is similar to the average cross-correlation in Fig. 3(a). This support the conclusion that the largest eigenvalue corresponds to the market mode described by numerous researches[19, 1] and it decreases when the value of q increases. Thus the market mode at small q is extremely stronger, which seems counterintuitive. We also observe that the first four eigenvalues increase as detrending scale s increases.

It is believed that those eigenvalues deviated from the prediction of random matrix theory contains some genuine information related to the sector or industry as described in Ref. [19, 21]. To uncover the hidden information carried by those deviating eigenvalues at different multifractal orders and detrending scales, we first partition the 401 stocks into industry groups labeled $l = 1 \dots 24$ (N_l stocks each) according to the industry group code of the stocks supplied by GICS. We then construct a projection matrix P , with elements $P_{li} = 1/N_l$ if stock i belongs to industry group l and $P_{li} = 0$ otherwise. For each eigenvector U_k , the contribution $X_k^l = \sum_{i=1}^N P_{li}(u_k^i)^2$ of each industry group can be obtained.

Fig 7 shows the contribution of each industry group to the smallest and second smallest eigenvalues $\lambda_k, k = 1, \lambda_k, k = 2$. The red ($k = 1$) and sky blue ($k = 2$) lines are the contribution value after the influence of the largest eigenvalue for λ_{401} is removed. The blue lines are the average contribution value X_k^l for the correlation matrices calculated using the shuffled time series. This reference model tells us how much the X_k^l deviate from the noise level. There are 24 major industry groups for the 401 stocks: **Media, Retailing, Consumer Durables&Apparel, Automobiles&Components, Consumer Services, Food&Beverage&Tobacco, Food&Staples Retailing, Household&Personal Products, Energy,**

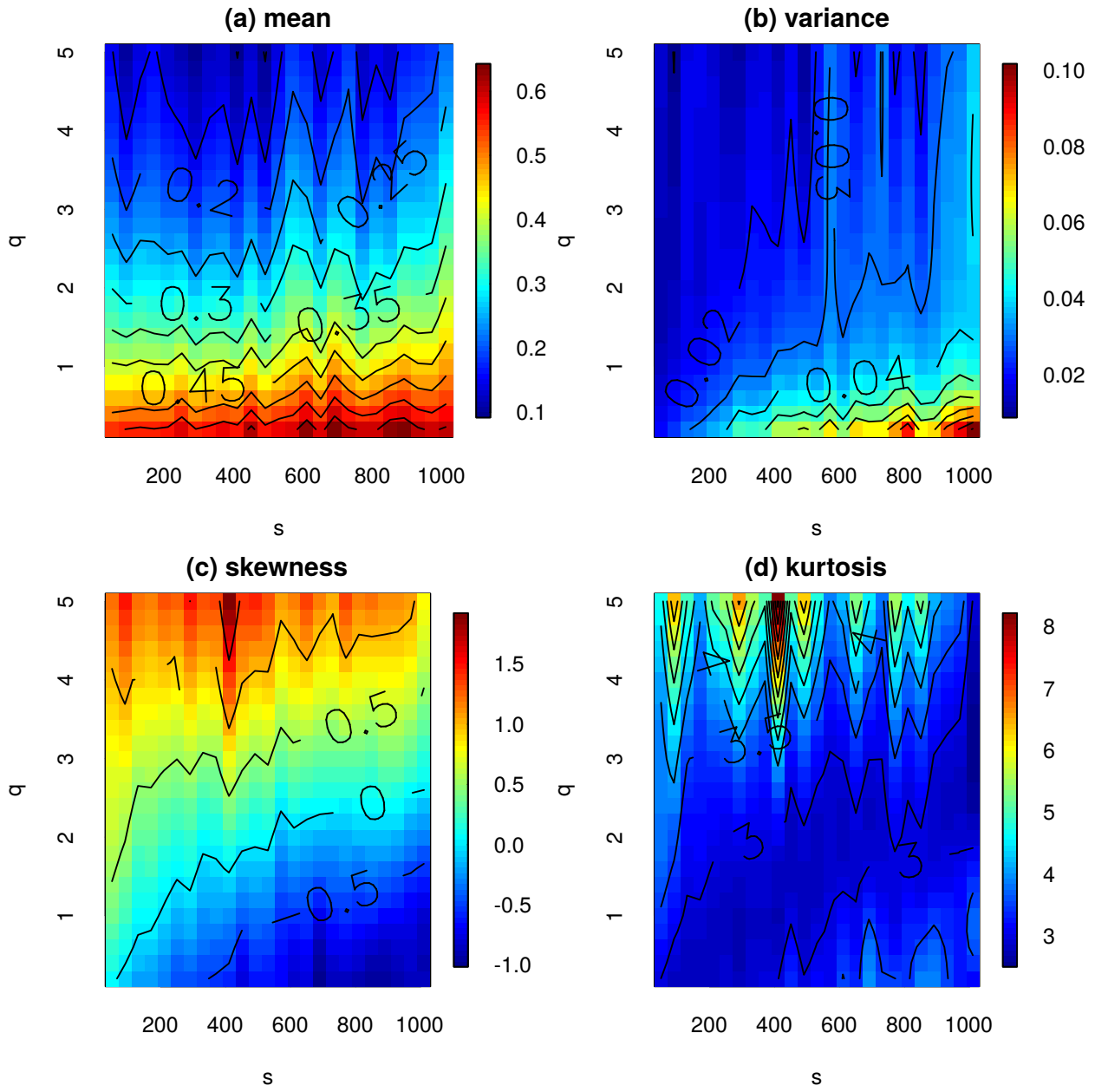


Figure 3: (Color on line) First four order moments: mean, variance, skewness, kurtosis of the correlation matrices at different multifractal order q and detrending scale s .

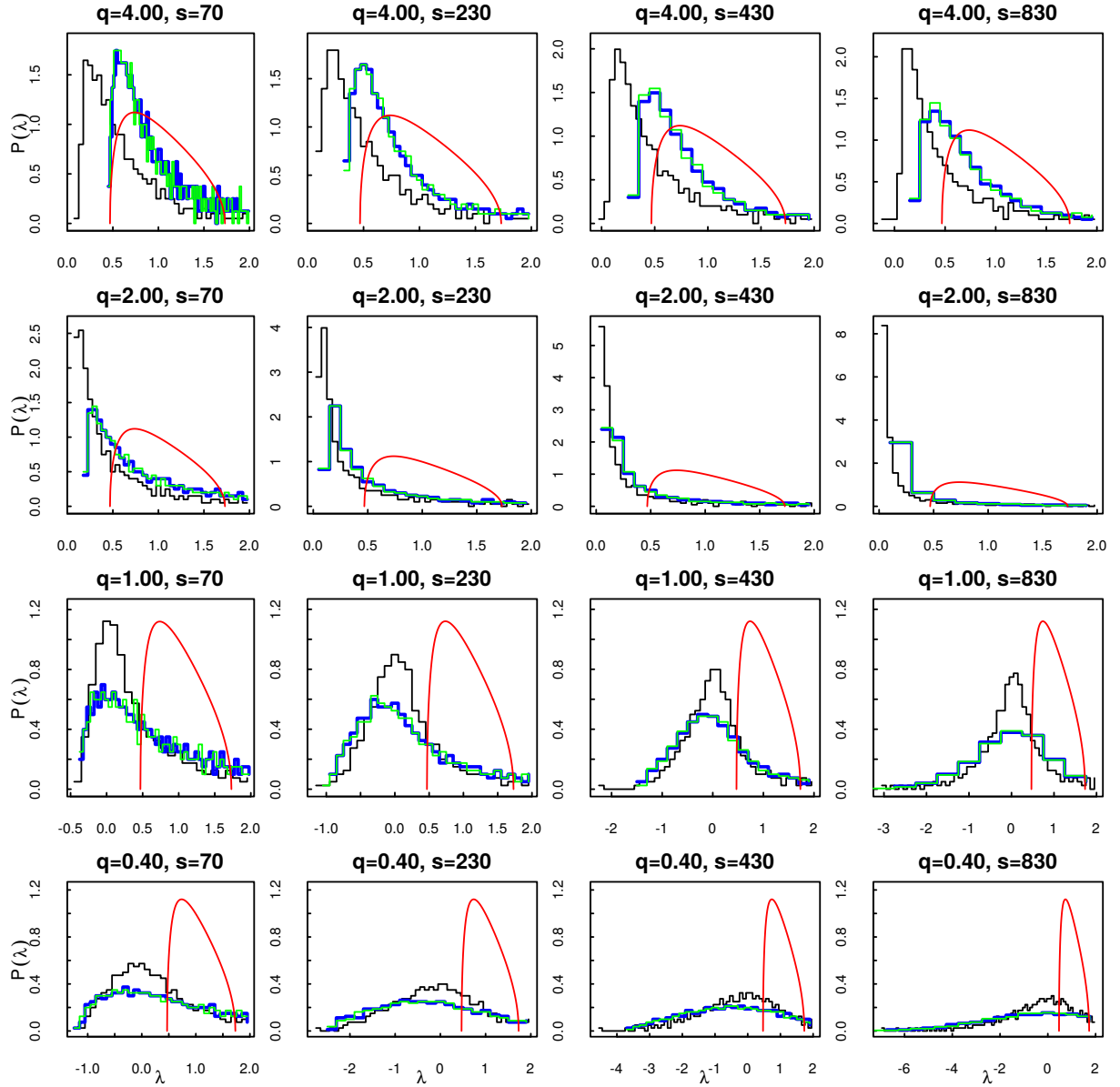


Figure 4: (Color on line) The eigenvalues distribution $P(\lambda)$ of the cross-correlation matrices inside the bulk. We only show the distribution of those eigenvalues smaller than 2. The black, blue and green lines are the eigenvalue distributions of the q -dependent cross-correlation matrices for the original, shuffled and simulated time series, respectively.

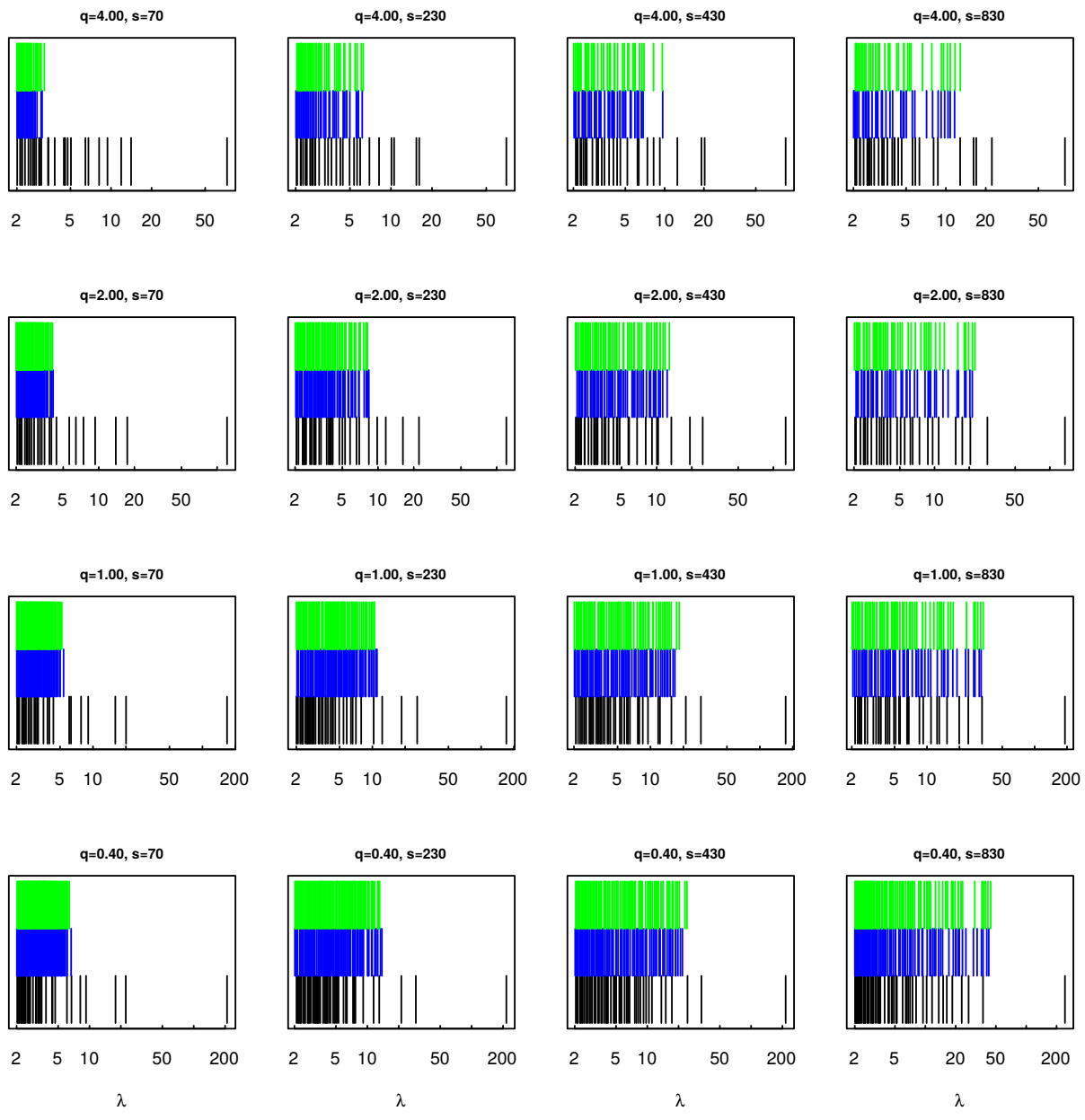


Figure 5: (Color on line) The eigenvalues of the cross-correlation matrices deviating from the bulk ($\lambda > 2$). The meaning of the color is the same as in Fig4.

Diversified Financials, Banks, Insurance, Real Estate, Pharmaceuticals, Biotechnology&Life Sciences, Health Care Equipment & Services, Capital Goods, Transportation, Software&Services, Commercial&Professional Services, Materials, Technology Hardware&Equipment, Semiconductors&Semiconductor Equipment, Telecommunication Services, Utilities, from left to right. It is shown that for the smallest and second smallest eigenvalues, λ_1 and λ_2 , the contribution come from a few industry groups and the X_k^l for these industry groups are much stronger than the noise level. The industry contribution of the large eigenvalues $\lambda_k, k = 399, 400$ are presented in Fig. 8. The contribution to large eigenvalues also come from a few industry groups and is much stronger than the noise level. For λ_{399} , there are multiple industry contribute significantly with a mixture pattern. The main contribution come from Diversified Financials, Banks, Real Estate and Utilities. But the contribution to λ_{400} always comes from Energy and Utilities.

As shown in Fig4, there are many small eigenvalues within the prediction of random matrix theory. Fig. 9 shows the contribution of each industry group to the eigenvalues $\lambda_k, k = 200, 250$ deep inside the eigenvalue bulk region. As expected, in this region the eigenvalues exhibit no significant pattern. The contribution level X_k^l of each industry group is the same as in the shuffled time series. For both $\lambda_k, k = 200$ and $\lambda_k, k = 250$, there are no clearly contributing industry groups.

As explained above, the inverse participate ratio quantifies the reciprocal of the number of eigenvector components that contribute significantly. Here we give the inverse participate ratio of the q -dependent cross-correlation matrices at different multifractal orders and detrending scales in Fig.10. We present the inverse participate ratio without the largest eigenvalue for better visualization. Note that there is a transition in the IPR I_k for small and large multifractal order q . When $q \leq 2$, the small eigenvalues are dominant by relatively small proportion of stocks with larger IPR. It can be validated using the participate ratio $1/I_k$ in Fig. 12, which is the participate ratio for those small eigenvalues less than 50. For medium and large eigenvalues the participate ratio are larger than 200.

Fig.11 shows the participate ratio $1/I_k$ for the largest eigenvalue. The largest participate ratio for $q < 2$ is 376 which approaches the system size $N = 401$. When $q \geq 2$, the participate ratio for largest eigenvalue decrease rapidly and has a value of 200. The striking difference in the contribution number of the largest eigenvalues for different fluctuations implies that the collective behavior of small fluctuations ($q < 2$) are more homogeneous (large participate ratio). Fig.12 shows the heat map of the participate ratio $1/I_k$ at different multifractal orders q when $s = 50, 210, 410, 810$. k is the label of the eigenvalue λ_k . When $q \geq 2$, the participate ratio for small eigenvalues (small k) are very small suggesting that the small eigenvalues contain useful information. Only a very small set of stocks contributed to the smallest eigenvalue. We can verify this using the eigenvector component contribution in Fig. 7. When $q \geq 2$ the small eigenvalues are dominated by a few sectors. This has implications relevant to portfolio optimization. In general, the pattern of collective behavior for small fluctuations differs from that of large fluctuations.

3.3. PMFG analysis

The planar maximally filtered graph (PMFG) has been used to analyze the structure and dynamics of stock market in times of crisis[30, 31], and it effectively captures the sector structures. Here we construct the PMFG networks using q -dependent cross-correlation matrices.

Fig 13 shows the networks constructed using PMFG algorithm. The sector structure for small q is clearer than those for large q . Recently Kawpen et al.[32] constructed the minimum spanning trees using the q -dependent cross-correlation matrices. Some hidden structures were found using minute datasets. Here we find that when $q \leq 2$, a hub stock emerges, but when $q > 2$, the degree heterogeneity becomes weak. Especially, when $q \leq 2$ the dark green nodes (the stocks form Financial sector) are very close with each other. However, when $q > 2$, the links between financial sector stocks loosen. Those characteristics qualitatively agree with the results from [32] in which they discover a star like minimum spanning tree structure when $q \leq 2$.

To quantify the influence of the fluctuations on the PMFGs at different multifractal orders q and detrending scales s , we calculate the topological quantities of the PMFGs. The topological quantities of the PMFGs are presented in Fig14. Fig14 (a) shows that the clustering coefficient C of PMFGs increases as the multifractal order q increases. The clustering coefficient is large when the detrending scale is short. The shortest path length L has been shown in Fig14(b). The shortest path length is large for large q and short s . Fig14 (c) is the heterogeneity index H [29], which quantifies the heterogeneity level of the PMFGs. It is analogous to the power law index of the scale-free network. It is known that the heterogeneity of BA network is 0.11. We notice that for small q the heterogeneity of the PMFG

network is larger than BA network. This means the structure of the PMFG networks for small multifractal orders q are extremely heterogeneous. we also show the assortativity A of the PMFGs at Fig14 (d). The negative assortativity for $q < 2$ gives a hint about the dis-assortative structure in which hub stocks tend to connect with the small degree stocks. When $q > 2$ the assortativity approaches 0. This indicates that for large q the connections are more evenly distributed(see Fig. 13). In a network with $q > 2$ the degree of the hub stocks are smaller than those hubs in networks with $q < 2$. From the variation of topological quantities, we can infer that for small fluctuations (small q) at short time scale (small s), there exist some leading stocks. But for large fluctuations (large q) and long time scale (large s), stocks are correlated uniformly. To sum up, from those topological quantities a obvious structure change is evident which gives an indication about the collective behaviors difference among fluctuations of different magnitudes at varying time scales.

4. Application

We are now exploring the possibility of using the q -dependent PMFG networks to improve the performance of portfolio optimization under the Markowitz portfolio framework[33]. First we briefly introduce the Markowitz portfolio theory and then we use some centrality metric to choose portfolio from the PMFG networks. Considering a portfolio $\Pi(t)$ of stocks with return $r_i, i = 1 \dots m$, m is the portfolio size, i.e., the number of stocks in the portfolio. The return on $\Pi(t)$ of stocks is

$$\Pi(t) = \sum_{i=1}^m \omega_i r_i(t),$$

where ω_i is the fraction of wealth invested in stock i . The fractions ω_i are normalized such that $\sum_{i=1}^m \omega_i = 1$. The risk in holding the portfolio $\Pi(t)$ can be quantified by the variance

$$\Omega^2 = \sum_{i=1}^m \sum_{j=1}^m \omega_i \omega_j C_{ij} \sigma_i \sigma_j,$$

here C_{ij} is the Pearson cross-correlation between r_i and r_j , and σ_i and σ_j are the standard deviations of r_i and r_j . To find an optimal portfolio, we maximize the return of the portfolio $\Phi = \sum_{t=1}^T \Pi(t)$ under the constraint that the risk on the portfolio is some fixed value Ω^2 . Maximizing Φ subject to these two constraints which is equivalent to a quadratic optimization problem

$$\omega^T \Sigma \omega - q * R^T \omega$$

Here Σ is the covariance matrix of the return matrix R mentioned in the previous context (now with dimension $L \times m$). The parameter q is the risk tolerance $q \in [0, \infty)$. If we set large q we have strong tolerance to the risk, which leads to large expected return. The optimal portfolios can be represented as a plot of the return Φ as a function of risk Ω^2 which is known as the efficient frontier. Here we do not use the q -dependent cross-correlation coefficient in the risk metric Ω^2 . We only use the q -dependent PMFG networks to select m stocks and then the traditional Markowitz portfolio theory is used to quantify the performance of the portfolio. It has shown that portfolio selected from the PMFG networks constructed from Pearson cross-correlation matrix using some centrality measures perform very well[34]. Here we first calculate the centrality scores defined by

$$\eta = \frac{C_D^w + C_D^u + C_{BC}^w + C_{BC}^u - 4}{4 \times (N - 1)} + \frac{C_E^w + C_E^u + C_C^w + C_C^u + C_{EC}^w + C_{EC}^u - 6}{6 \times (N - 1)}$$

where C_D^w is the ranking of weighted Degree (D) and C_D^u is its unweighted counterpart. The other centrality metrics are Betweenness Centrality (BC), Eccentricity (E), Closeness (C), Eigenvector Centrality (EC). A portfolio construct

using the central (peripheral) stocks are those with very high (low) centrality value η . A complete description of this composed centrality metric is provided in Ref.[34]. Actually, the choice of the centrality metric does not significantly effect the final results. Here in Fig.15, we show the efficient frontiers calculated from those portfolio constructed using central (black lines), peripheral (red lines) and random (blue lines) stocks with different multifractal orders q . We have tested on the portfolio size $m = 10, 20, 30, 40, 50, 60$ and calculated the average return value for all the detrending scales s at one specific risk value to show the effect of fluctuations at different magnitudes. It is very clear that for different portfolio size from 10 to 60 stocks, the peripheral portfolio (red lines) are always the best performed. The performance of the central portfolio is even worse than the random portfolio.

We then calculate the return difference between peripheral and central portfolio $\Delta = \Phi_p - \Phi_c$ (p and c are peripheral and central portfolios, respectively) as a function of the multifractal order q in Fig.16. Here we use multifractal orders from 0.2 to 10 to identify the optimal q . It's very obvious that the peripheral portfolio outperforms the central portfolio most around multifractal order $q = 2$ and exhibits a greater than %7 superiority. This may gives a hint that we should trade based on moderate fluctuation with higher return and lower risk. The results above indicate the potential of utilizing the q -dependent cross-correlation matrix as a new portfolio optimization tool.

5. Conclusion

In this paper, we have employed the q -dependent cross-correlation coefficient to analyze the cross-correlation among fluctuations at different magnitudes for stock market. With the help of random matrix theory and complex network theory, we analyze the cross-correlation matrices of the stock market for different magnitude of fluctuations. We find that the cross-correlation among small fluctuations are stronger than large ones. There are more deviating eigenvalues for large fluctuations than that for small fluctuations. Analyzing the inverse participate ratio and the eigenvector contribution, we find that the small eigenvalues of the cross-correlation matrices for large fluctuations are dominated by a small number of industry groups. This is similar to those large deviating eigenvalues that are also dominated by a small number of industry groups. Thus we conclude that small eigenvalues of the q -dependent cross-correlation matrices also carry some genuine information, which seems very counterintuitive. The complex network representation have also validate the correlation difference between small and large fluctuations. The network structure are more heterogeneous and dis-assortativity for the network constructed from small fluctuations which means the existence of leading stocks for small fluctuations. We then utilize the network centrality as a portfolio selection metric. Under the Markowitz portfolio theory, we find that the portfolio of the peripheral stocks always outperforms the portfolio of central stocks. Optimal multifractal order q with the largest return difference approaching %7 is approximately $q = 2$. This may be used as a new portfolio optimization tool. Thus our investigation about the cross-correlation among stocks with different magnitude of fluctuations have demonstrated the huge difference between large and small fluctuations of stock market. They are regulated by different non-linear correlation structures. Those results expands our understanding of the collective behavior of the stock market.

6. Acknowledgments

This work is supported in part by the Programme of Introducing Talents of Discipline to Universities under grant NO. B08033 and and the program of China Scholarship Council (No. 201606770023).

References

- [1] Vasiliki Plerou, Parameswaran Gopikrishnan, Bernd Rosenow, Luís Nunes Amaral, and H. Stanley. Universal and Nonuniversal Properties of Cross Correlations in Financial Time Series. *Physical Review Letters*, 83(7):1471–1474, 1999.
- [2] Laurent Laloux, Pierre Cizeau, Jean-Philippe Bouchaud, and Marc Potters. Noise Dressing of Financial Correlation Matrices. *Physical Review Letters*, 83(7):1467–1470, aug 1999.
- [3] C. K. Peng, S. V. Buldyrev, S. Havlin, M. Simons, H. E. Stanley, and a. L. Goldberger. Mosaic organization of DNA nucleotides. *Physical Review E*, 49(2):1685–1689, 1994.
- [4] Boris Podobnik and H. Stanley. Detrended Cross-Correlation Analysis: A New Method for Analyzing Two Nonstationary Time Series. *Physical Review Letters*, 100(8):084102, feb 2008.
- [5] Jan W. Kantelhardt, Stephan a. Zschiegner, and H. Eugene Stanley. Multifractal detrended uctuation analysis of nonstationary time series. *Physica A*, 316:87–114, 2002.

- [6] Wei-Xing Zhou. Multifractal detrended cross-correlation analysis for two nonstationary signals. *Physical Review E*, 77(6):066211, jun 2008.
- [7] Paweł Oświecimka, Stanisław Drożdż, Marcin Forczek, Stanisław Jadach, and Jarosław Kwapien. Detrended cross-correlation analysis consistently extended to multifractality. *Physical Review E*, 89(2):023305, feb 2014.
- [8] Boris Podobnik, Zhi Qiang Jiang, Wei Xing Zhou, and H. Eugene Stanley. Statistical tests for power-law cross-correlated processes. *Physical Review E - Statistical, Nonlinear, and Soft Matter Physics*, 84:1–8, 2011.
- [9] Hadrien Salat, Roberto Murcio, and Elsa Arcaute. Multifractal methodology. *Physica A*, 473:1–14, 2016.
- [10] Longfeng Zhao, Wei Li, Chunbin Yang, Jihui Han, Zhu Su, and Yijiang Zou. Multifractality and Network Analysis of Phase Transition. *PLOS ONE*, 12(1):1–23, 2017.
- [11] G.F. Zebende. DCCA cross-correlation coefficient: Quantifying level of cross-correlation. *Physica A: Statistical Mechanics and its Applications*, 390(4):614–618, feb 2011.
- [12] Ladislav Kristoufek. Measuring correlations between non-stationary series with DCCA coefficient. *Physica A: Statistical Mechanics and its Applications*, 402:291–298, may 2014.
- [13] Gang-Jin Wang, Chi Xie, Shou Chen, Jiao-Jiao Yang, and Ming-Yan Yang. Random matrix theory analysis of cross-correlations in the US stock market: Evidence from Pearson’s correlation coefficient and detrended cross-correlation coefficient. *Physica A: Statistical Mechanics and its Applications*, 392(17):3715–3730, sep 2013.
- [14] Gang-Jin Wang, Chi Xie, Yi-Jun Chen, and Shou Chen. Statistical Properties of the Foreign Exchange Network at Different Time Scales: Evidence from Detrended Cross-Correlation Coefficient and Minimum Spanning Tree. *Entropy*, 15(5):1643–1662, 2013.
- [15] G.F. Zebende, M.F. da Silva, and A. Machado Filho. DCCA cross-correlation coefficient differentiation: Theoretical and practical approaches. *Physica A: Statistical Mechanics and its Applications*, 392(8):1756–1761, apr 2013.
- [16] Xuelian Sun and Zixian Liu. Optimal portfolio strategy with cross-correlation matrix composed by DCCA coefficients: Evidence from the Chinese stock market. *Physica A: Statistical Mechanics and its Applications*, 444:667–679, 2016.
- [17] Jarosław Kwapien, Paweł Oświecimka, and Stanisław Drożdż. Detrended fluctuation analysis made flexible to detect range of cross-correlated fluctuations. *Physical review. E, Statistical physics, plasmas, fluids, and related interdisciplinary topics*, 052815:1–11, 2015.
- [18] M Tumminello, T Aste, T Di Matteo, and R N Mantegna. A tool for filtering information in complex systems. *Proceedings of the National Academy of Sciences of the United States of America*, 102(30):10421–6, July 2005.
- [19] Parameswaran Gopikrishnan, Bernd Rosenow, Vasiliki Plerou, and H Stanley. Quantifying and interpreting collective behavior in financial markets. *Physical Review E*, 64(3):1–4, 2001.
- [20] B. Rosenow, V. Plerou, P. Gopikrishnan, and H. E. Stanley. Portfolio Optimization and the Random Magnet Problem. *Europhysics Letters*, 59(4):500–506, 2002.
- [21] Vasiliki Plerou, Parameswaran Gopikrishnan, Bernd Rosenow, Luís Amaral, Thomas Guhr, and H. Stanley. Random matrix approach to cross correlations in financial data. *Physical Review E*, 65(6):066126, jun 2002.
- [22] B. Podobnik, D. Wang, D. Horvatic, I. Grosse, and H. E. Stanley. Time-lag cross-correlations in collective phenomena. *EPL (Europhysics Letters)*, 90:68001, 2010.
- [23] Wei-Xing Zhou, Guo-Hua Mu, and János Kertész. Random matrix approach to the dynamics of stock inventory variations. *New Journal of Physics*, 14(9):093025, sep 2012.
- [24] Giacomo Livan, Simone Alfarano, and Enrico Scalas. Fine structure of spectral properties for random correlation matrices: An application to financial markets. *Physical Review E*, 84(1):016113, jul 2011.
- [25] Daniel J. Fenn, Mason a. Porter, Stacy Williams, Mark McDonald, Neil F. Johnson, and Nick S. Jones. Temporal evolution of financial-market correlations. *Physical Review E*, 84(2):026109, August 2011.
- [26] Duan Wang, Boris Podobnik, Davor Horvatić, and H. Eugene Stanley. Quantifying and modeling long-range cross correlations in multiple time series with applications to world stock indices. *Physical Review E*, 83(4):046121, apr 2011.
- [27] Ajay Singh and Dinghai Xu. Random matrix application to correlations amongst the volatility of assets. *Quantitative Finance*, 16(1):69–83, 2015.
- [28] Joël Bun, Jean-Philippe Bouchaud, and Marc Potters. Cleaning large correlation matrices: Tools from random matrix theory. *Physics Reports*, 666:1–109, 2016.
- [29] Ernesto Estrada. Quantifying network heterogeneity. *Physical Review E*, 82(6):66102, 2010.
- [30] Dong-Ming Song, Michele Tumminello, Wei-Xing Zhou, and Rosario N. Mantegna. Evolution of worldwide stock markets, correlation structure, and correlation-based graphs. *Physical Review E*, 84(2):026108, aug 2011.
- [31] Longfeng Zhao, Wei Li, and Xu Cai. Structure and dynamics of stock market in times of crisis. *Physics Letters A*, 1:1–13, 2015.
- [32] Jarosław Kwapien, Paweł Oświecimka, Marcin Forczek, and Stanisław Drożdż. Minimum spanning tree filtering of correlations for varying time scales and size of fluctuations. pages 1–8, 2016.
- [33] Harry Markowitz. Portfolio Selection. *The Journal of Finance*, 7(1):77, mar 1952.
- [34] F Pozzi, T Di Matteo, and T Aste. Spread of risk across financial markets: better to invest in the peripheries. *Scientific reports*, 3:1665, 2013.

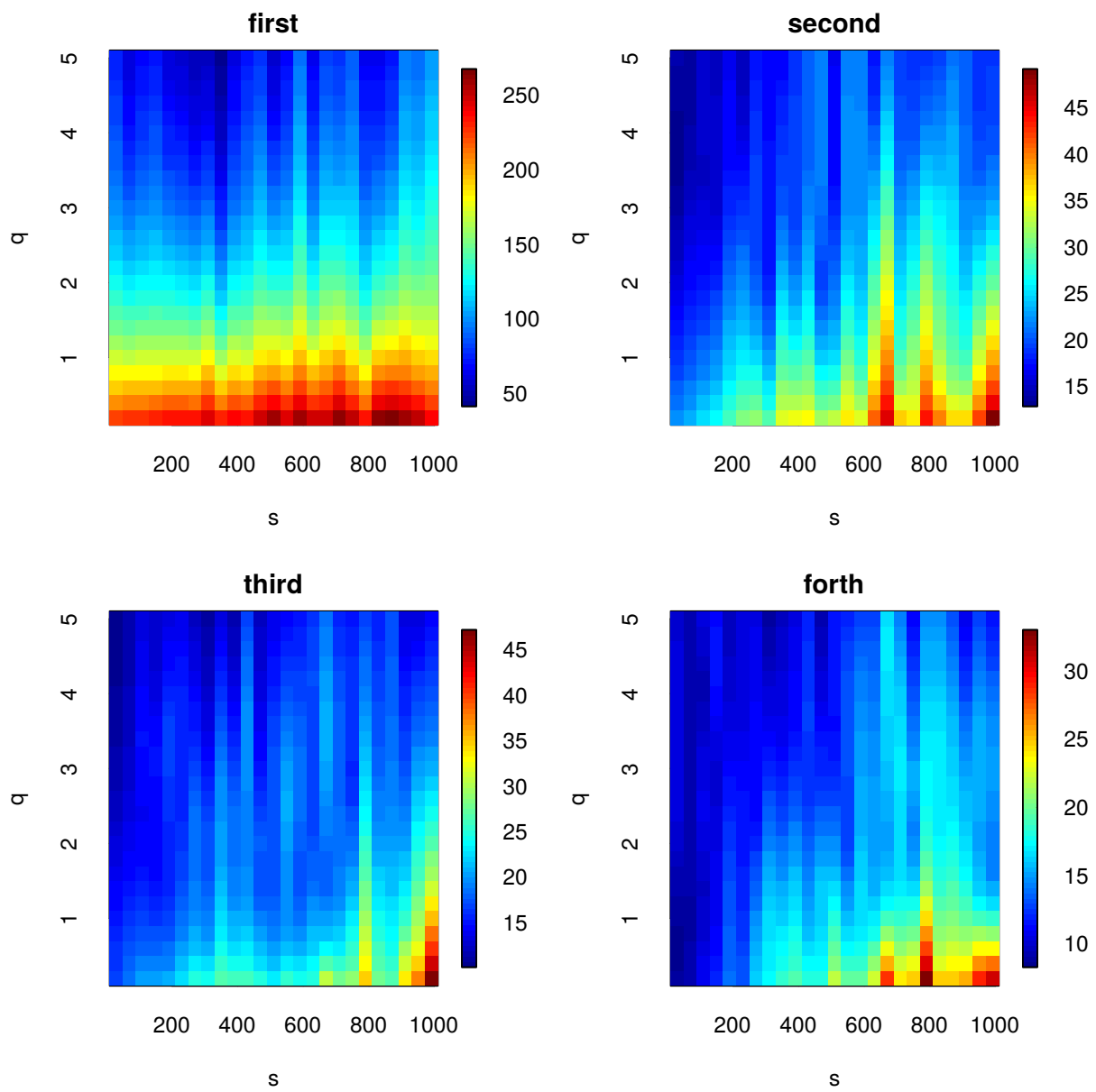


Figure 6: (Color on line) The first four eigenvalues $\lambda_k, k = 1 \dots 4$ as a function of multifractal order q and detrending scale s .

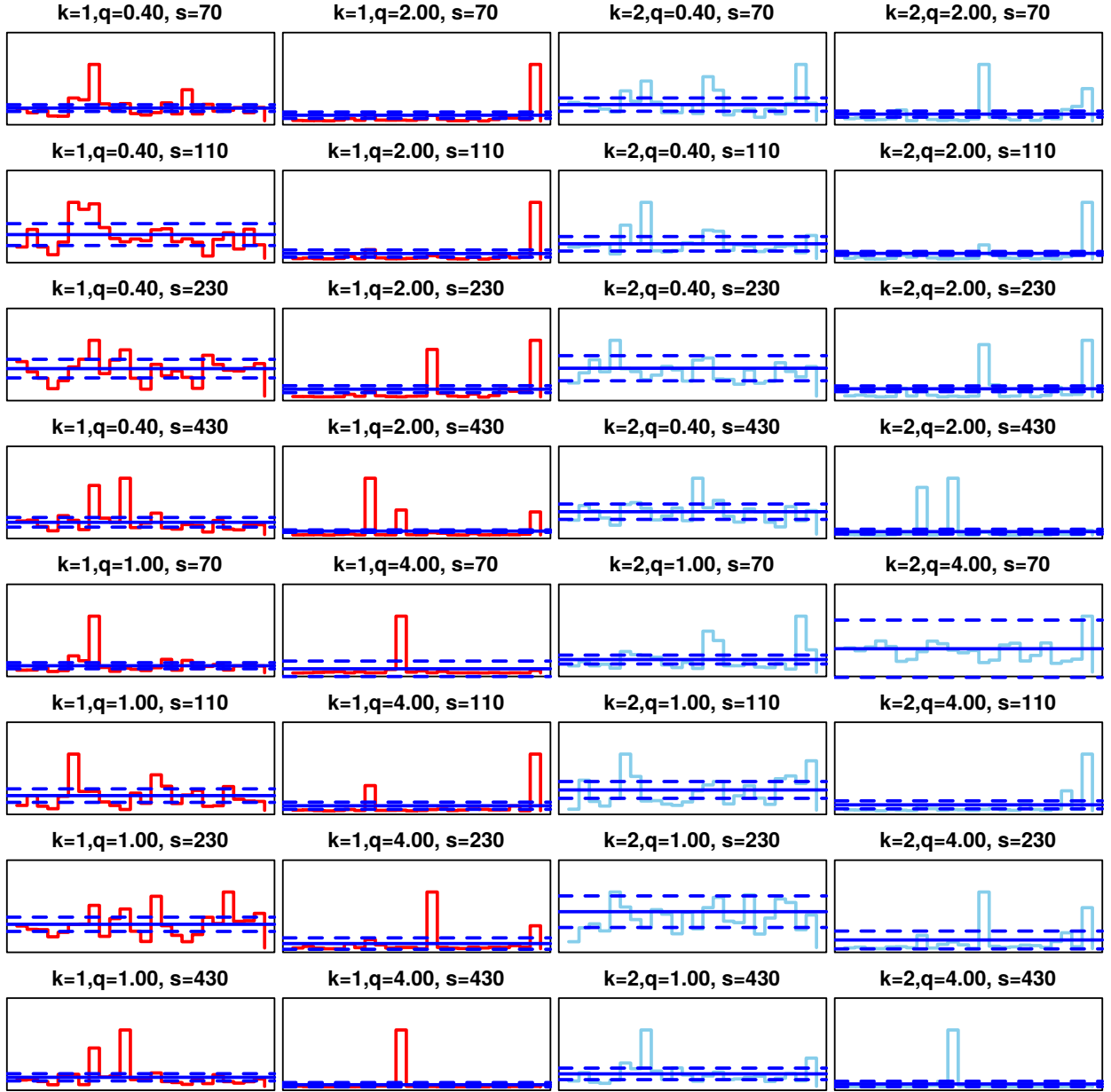


Figure 7: (Color on line) The contribution $X_k^l, l = \dots, 24$ of every industry group to the smallest eigenvalue $\lambda_k, k = 1$ (red lines) and second smallest eigenvalue $\lambda_k, k = 2$ (sky blue lines) at different multifractal order q and detrending scale s . The blue solid and dashed lines are the mean X_k^l with one standard deviation for the shuffled correlation matrices.

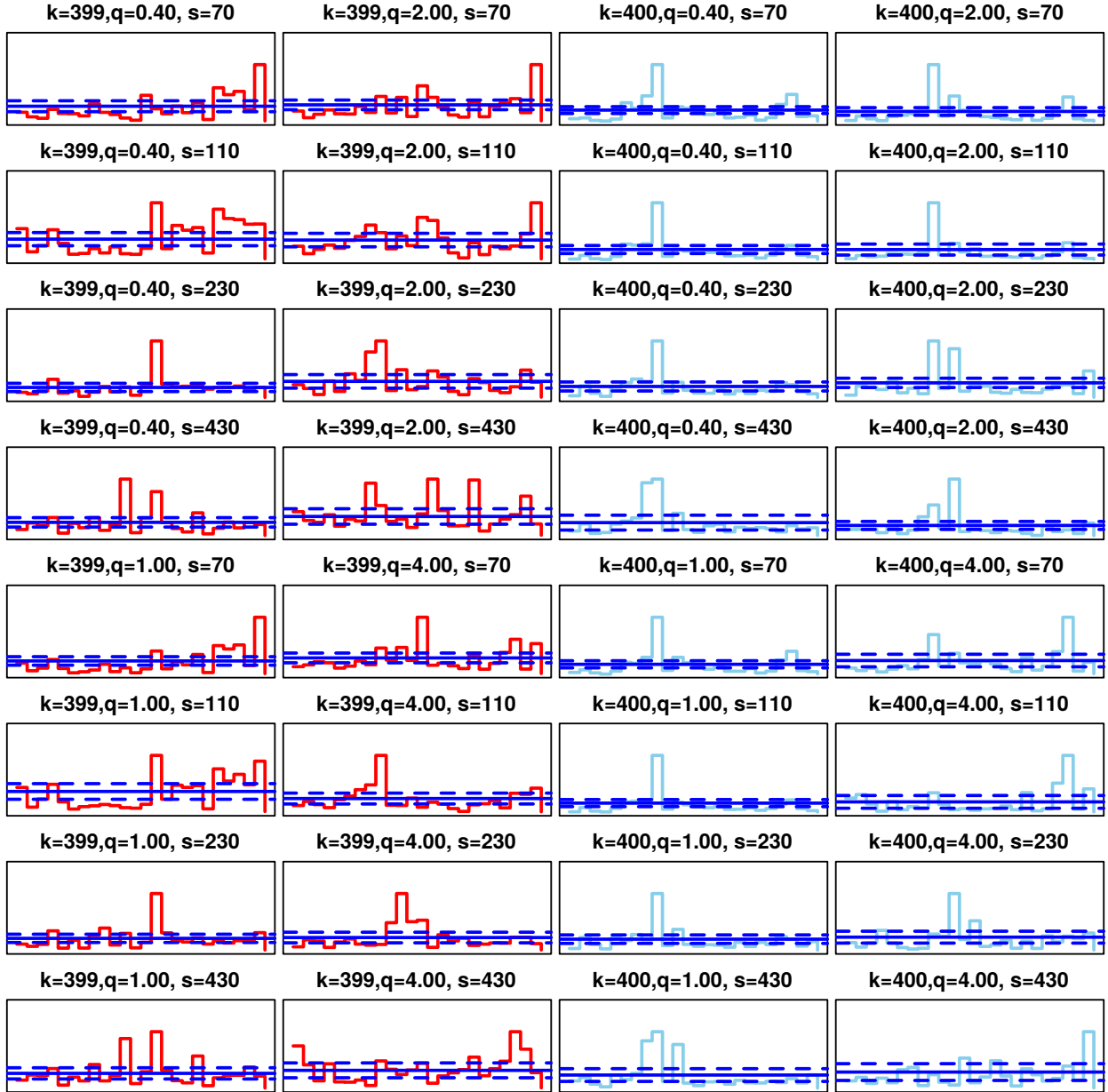


Figure 8: (Color on line) The contribution $X_k^l, l = 1 \dots 24$ of every industry group to the third largest eigenvalue $\lambda_k, k = 399$ (red lines) and second largest eigenvalue $\lambda_k, k = 400$ (sky blue lines) at different multifractal order q and detrending scale s . The blue solid and dashed lines are the mean X_k^l with one standard deviation for the shuffled correlation matrices.

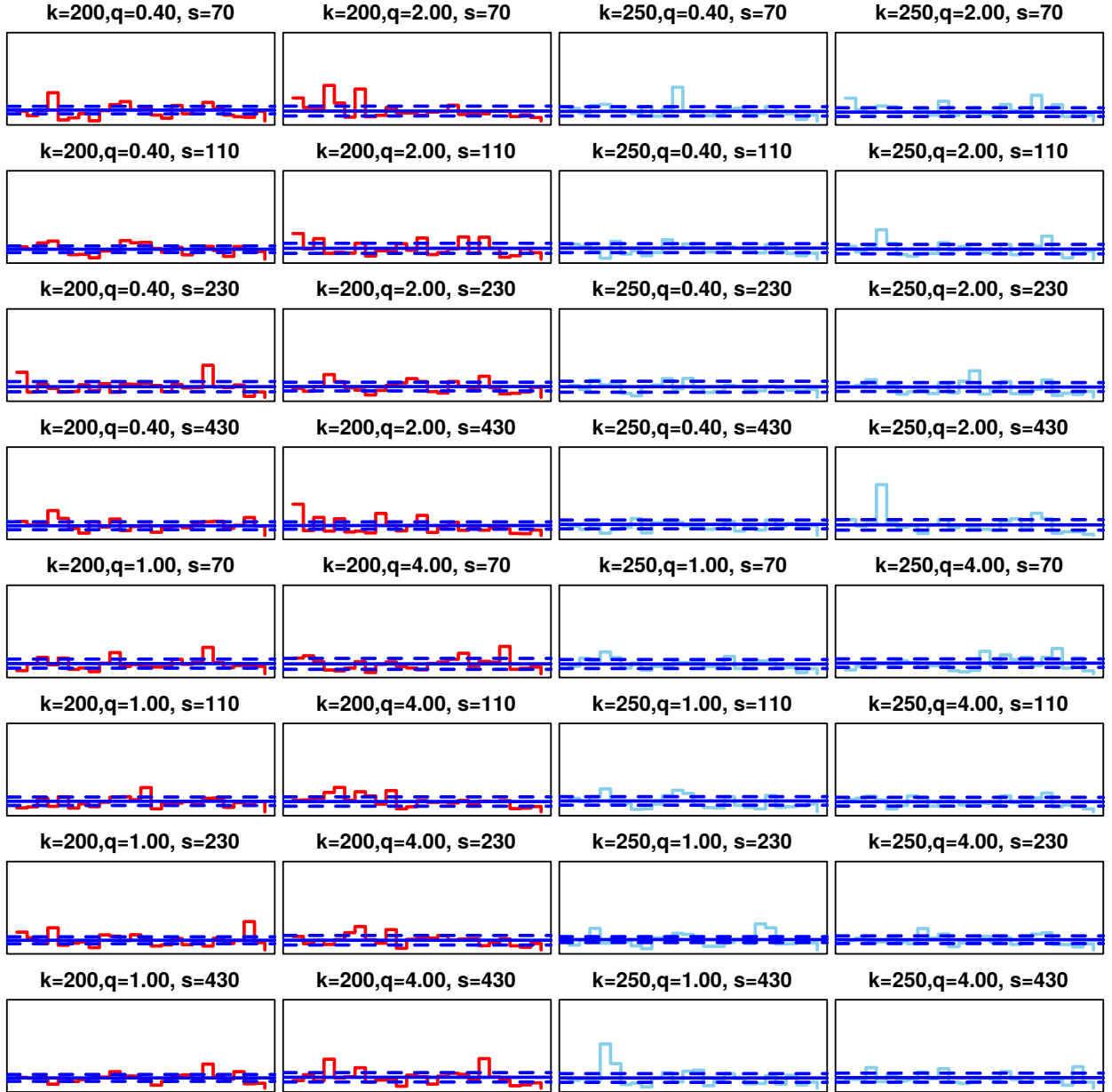


Figure 9: (Color on line) The contribution $X_k^l, l = \dots, 24$ of each industry group to those eigenvalues fall deep inside the bulk $\lambda_k, k = 200$ (red lines) and $\lambda_k, k = 250$ (sky blue lines) at different order q and detrending scale s . The blue solid and dashed lines are the mean X_k^l with one standard deviation for the shuffled correlation matrices.

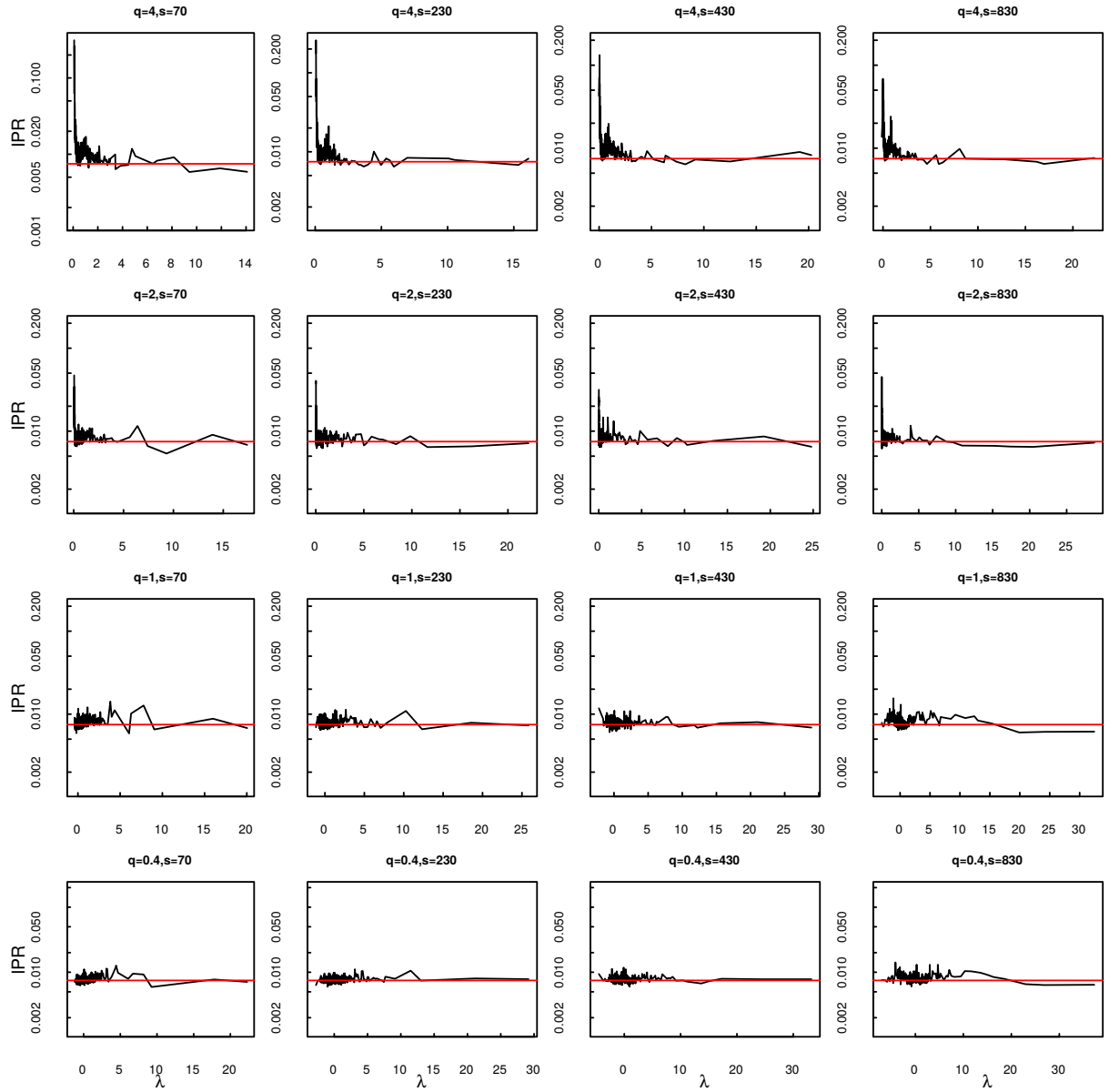


Figure 10: (Color on line) The inverse participate ratio (IPR) as a function of eigenvalues with out the largest eigenvalue for different multifractal order q and detrending scale s . The red line is the inverse participate ratio for random matrix with value $\langle I_k \rangle = 3/N$.

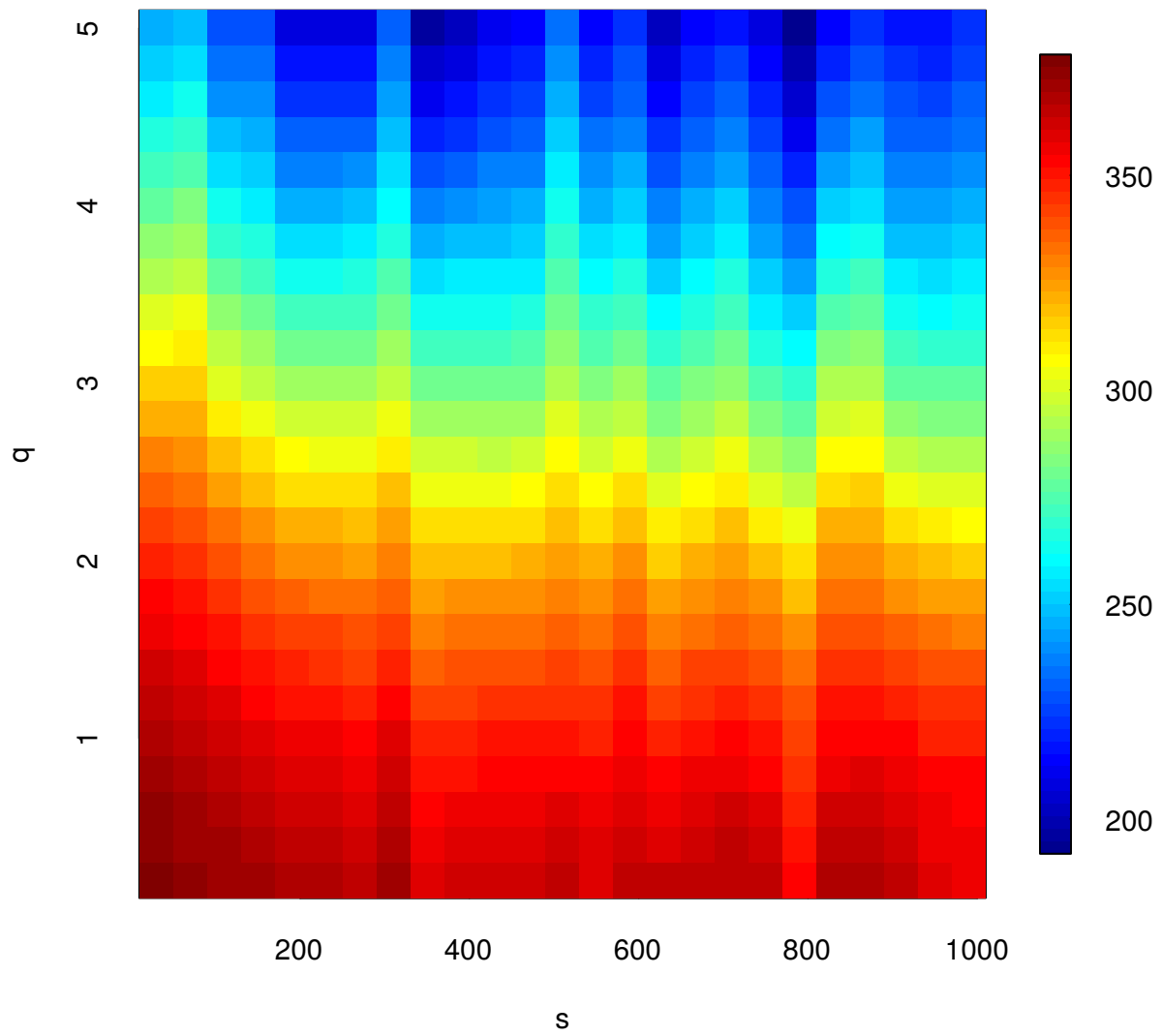


Figure 11: (Color on line) The participate ratio(PR) $1/I_k$ of the largest eigenvalue λ_{401} for different multifractal order q and detrending scale s .

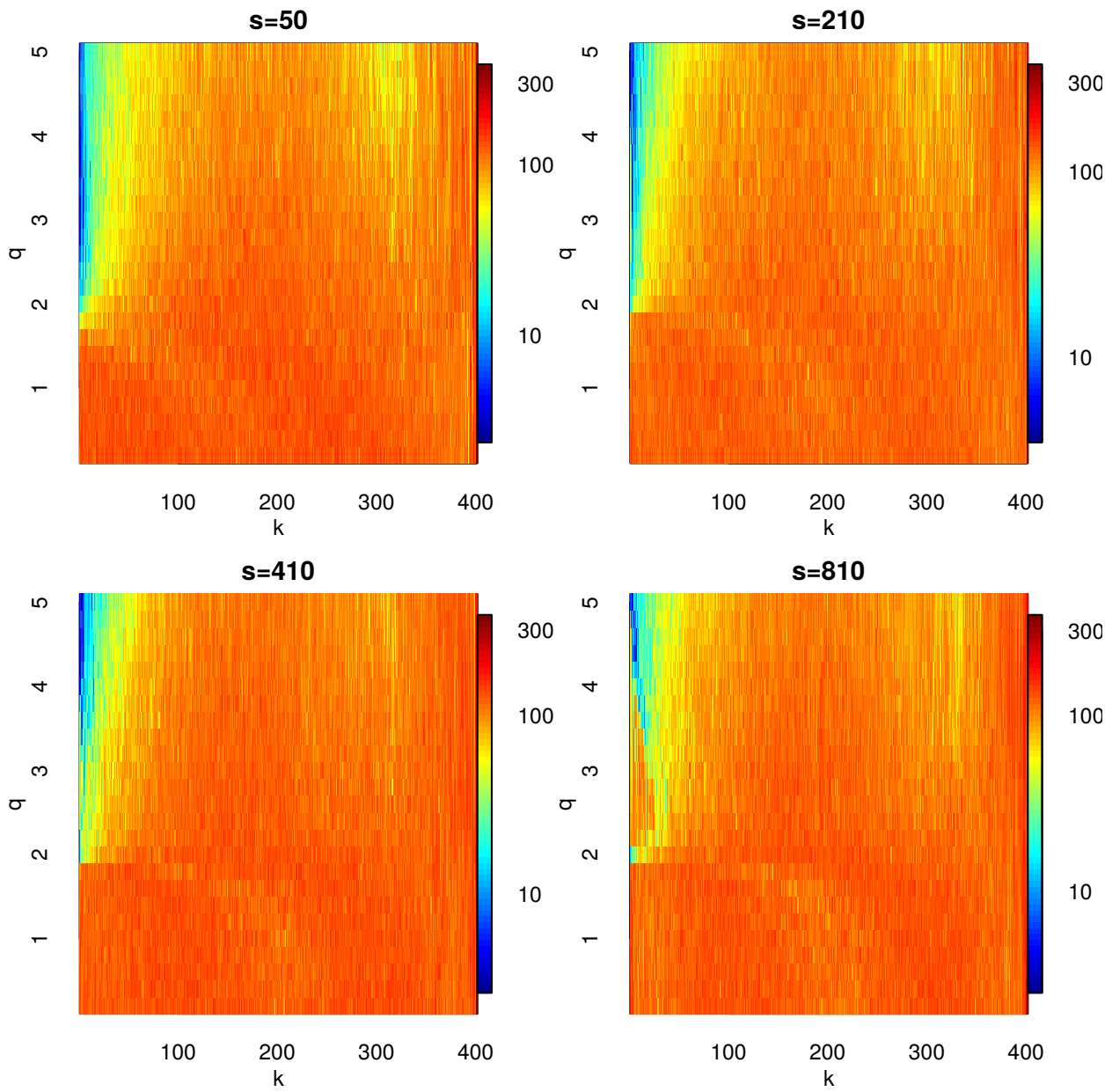


Figure 12: (Color on line) The participate ratio $1/I_k$ as a function of q and k . k is the label of the eigenvalues λ_k . Here we set detrending scale $s = 50, 210, 410, 810$.

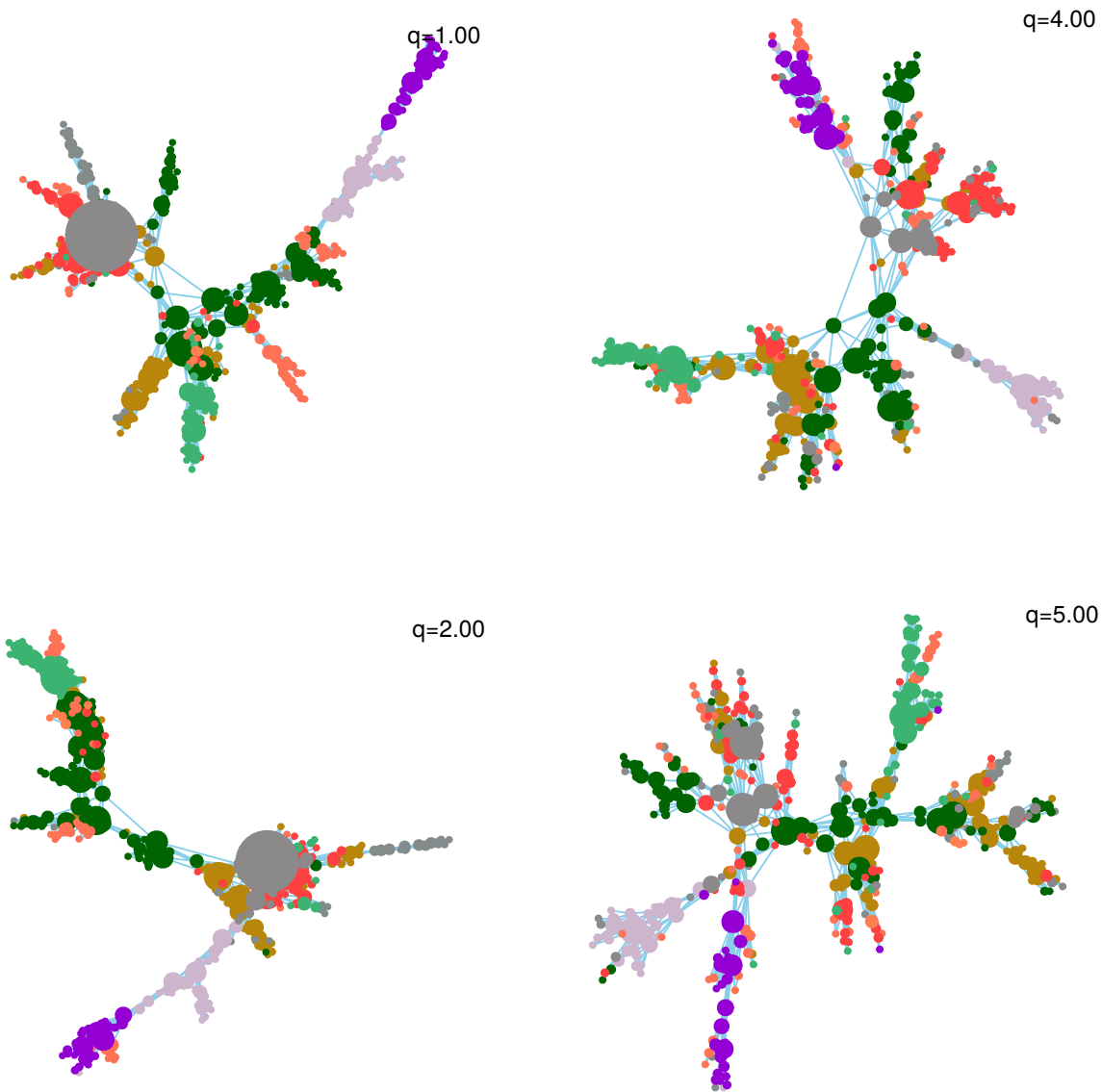


Figure 13: (Color on line) The PMFG networks for different orders q . We set detrending scale $s = 110$ here. Different vertex colors represent different sectors. The vertex size is proportion to the degree of each vertex.

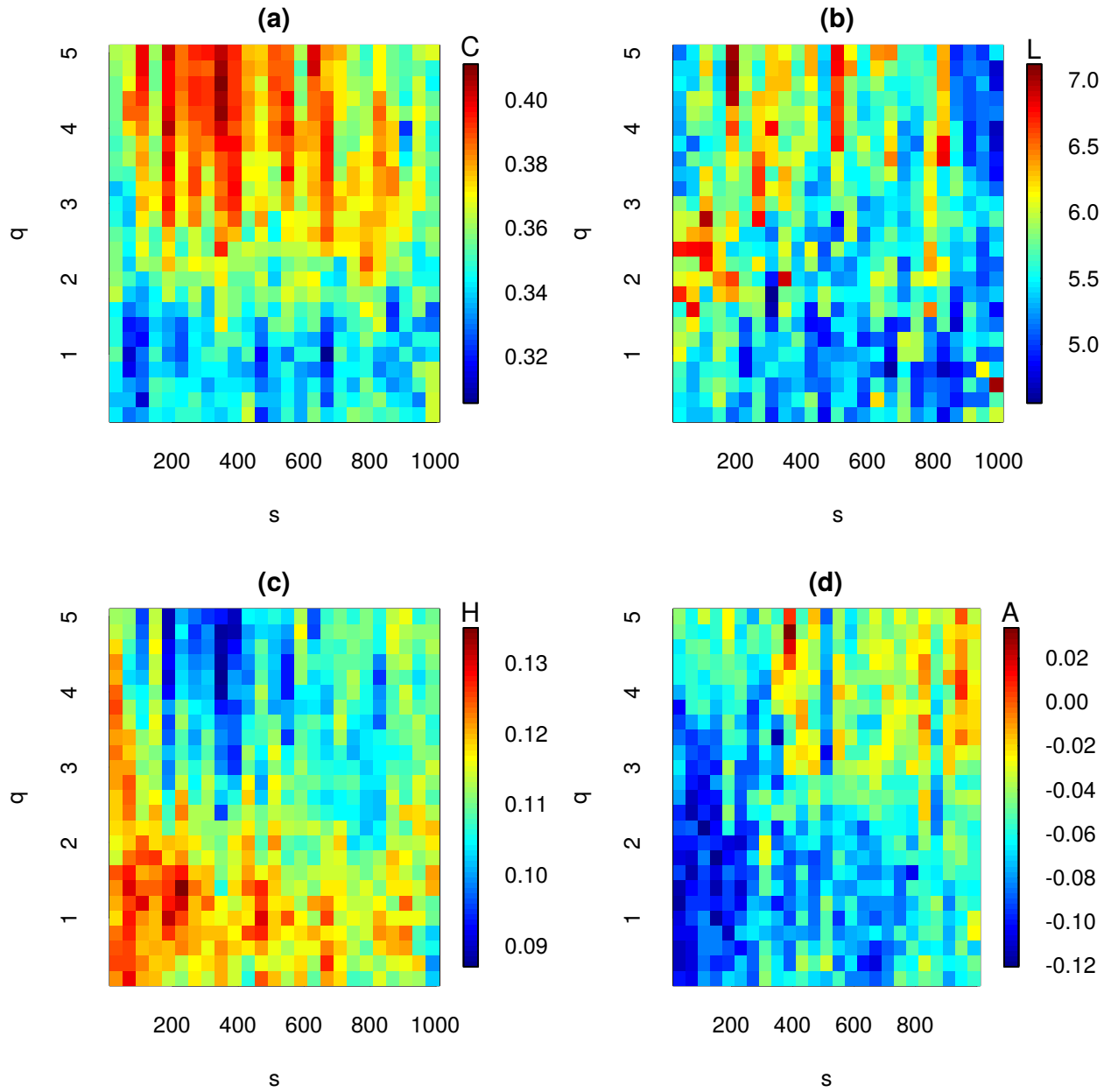


Figure 14: (Color on line) The topological quantities of the PMFGs at different order q and scale s . (a) is the clustering coefficient C , (b) is the shortest path length L , (c) is the heterogeneity index H , (d) is the assortativity A .

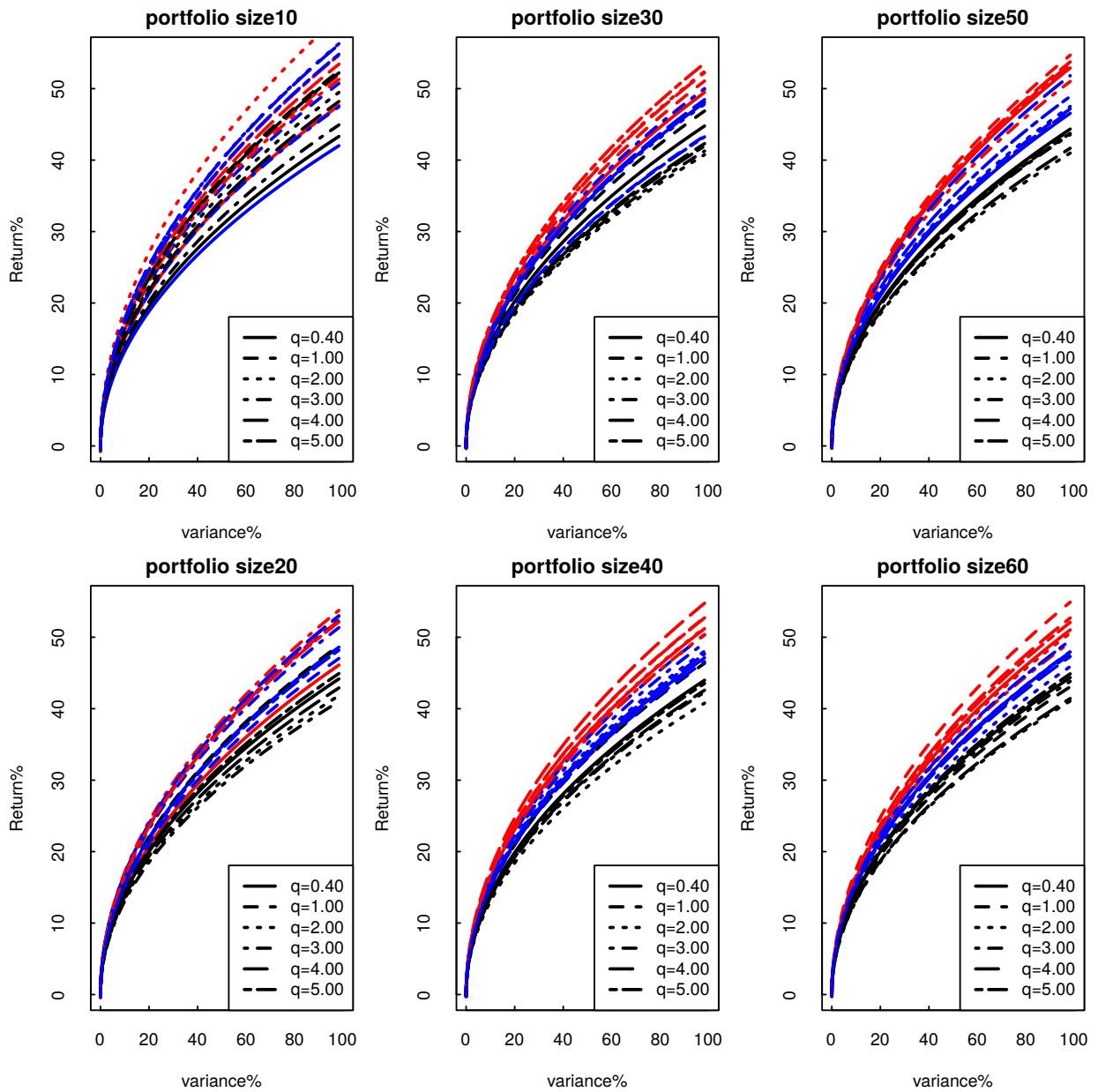


Figure 15: (Color on line) The efficient frontier for different portfolio size $m = 10, 20, 30, 40, 50, 60$. The red, blue and black lines are efficient frontiers for those portfolio constructed using peripheral, random selected and central stocks in the PMFG networks.

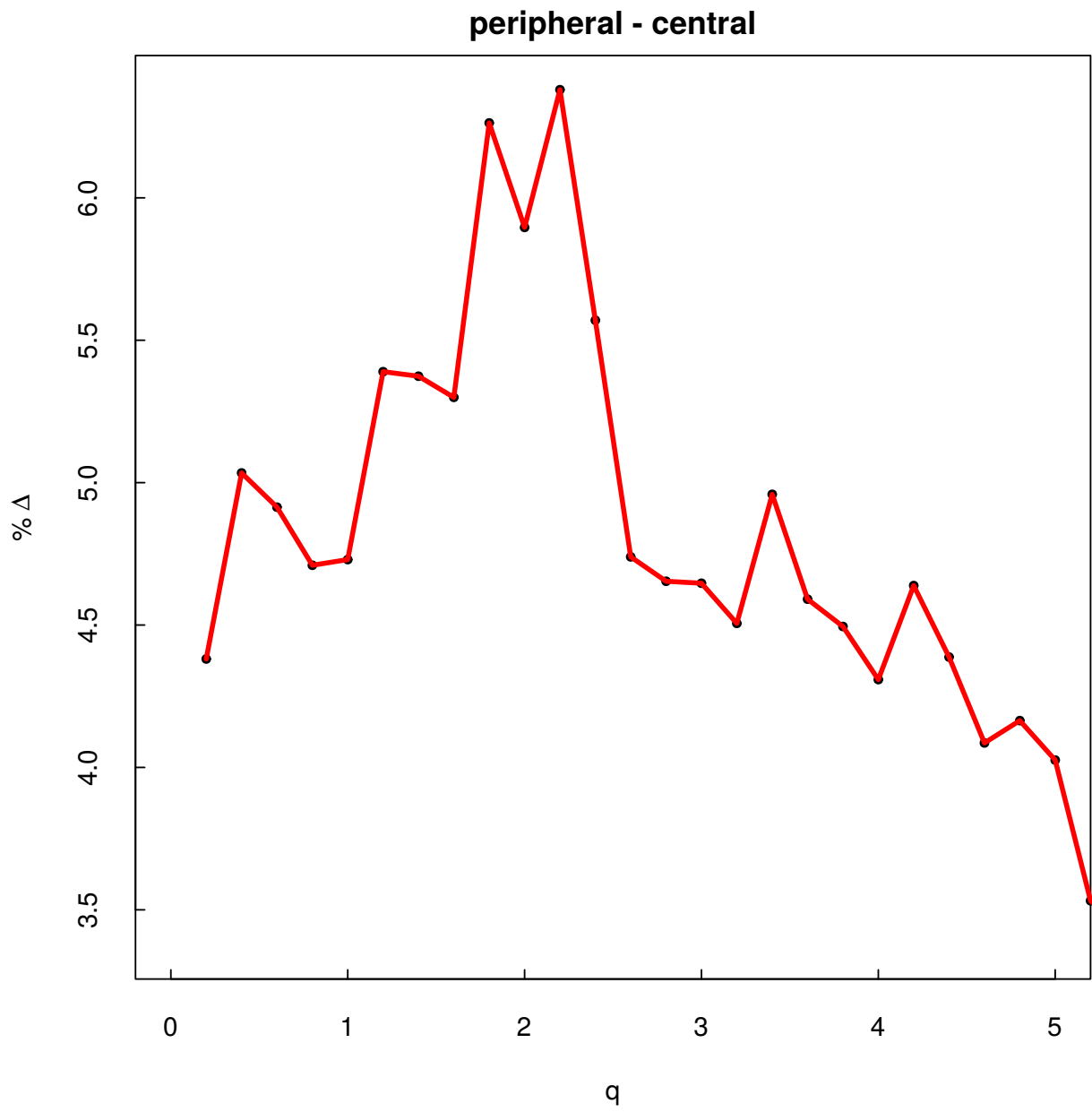


Figure 16: (Color on line) The difference between the return of peripheral and the return of central portfolio as a function of multifractal order q .